ENERGETIKA. 2004. Nr. 4. P. 12–18

Finite element analysis of thermal fields in the pulsed power magnetic field generator

Vincas Ðnirpûnas,
Eugeniuð Stupak,
Rimantas Kaèianauskas

Vilnius Gediminas Technical University, Department of Strength of Materials, Saulëtekio al. 11, LT-10223 Vilnius

Arnas Kaèeniauskas

Vilnius Gediminas Technical University, Parallel Computing Laboratory, Saulëtekio 11, LT-10223 Vilnius

Jurij Novickij

Vilnius Gediminas Technical University, Vilnius High Magnetic Field Centre, A. Goštauto g. 11, LT-01108 Vilnius

The paper presents a finite element analysis of thermal fields in a pulsed power magnetic field generator. The laboratory system developed at the Vilnius High Magnetic Field Centre generates half-period sinus-shaped magnetic field pulses of 2 ms duration and with amplitudes up to 50 T. The peak power of the designed generator is up to 15 MW. Numerical analysis performed by the finite element method simulated the transient behaviour of magnetic fluxes, induced heat and thermal fields in the pulsed generator. The non-linear thermal analysis was performed considering temperature-dependent specific heat and conductivity. The numerical behaviour of magnetic fields was validated by comparison with experimental measurements, while thermal analysis served for prediction of the temperature-dependent material properties.

Key words: thermal analysis, coupled magneto-thermal analysis, pulsed power magnetic field generators, the finite element method

1. INTRODUCTION

Pulsed power technologies are important investigation tools used in many fields of applied sciences and engineering. For scientific investigations, especially in the field of pulsed power engineering, it is necessary to have compact, secure pulsed power magnetic field generators that can be easily used under laboratory conditions [1]. Pulsed power electromagnetic research is successfully applied to nuclear energy applications [2]. Recently, attention has been focused on small-size magnetic flux generators producing high magnetic field pulses with a short rise and decay time [3]. At the Vilnius High Magnetic Field Centre, in close collaboration with Vilnius Gediminas Technical University and Semiconductor Physics Institute, such generators of high magnetic fields are developed [4]. The peak power of the pulsed device varies from 1 to 15 MW.

The design and construction of pulsed power devices is a complicated technical problem including analysis of multiphysical phenomena [5]. Electrically, an inductive coil is just a heater – indeed the most powerful ever built. The current induces the Joule heat in the coil windings, which quickly raises the temperature of the solenoid [6]. The temperature field influences the mechanical properties [7] of the construction which is loaded by very large forces generated by high magnetic fields.

Maxwell's partial differential equations represent a fundamental unification of electric and magnetic fields predicting electromagnetic phenomena in pulsed generators. Although analytical solutions of Maxwell equations exist for simple geometries, solutions of these equations for a vast majority of engineering problems have to be sought through computational simulations. The finite element method has emerged as a valuable tool for solution of various problems in the area of structural mechanics [8]. Later the range of applicability of the method was extended to the problems of heat transfer [9] as well as to electrical problems [10]. The 3D static FEM analysis of Maxwell's equations was performed by Demerdash [11]. The scalar potential formulation of Maxwell's equations was proposed in [12]. The solution of 3D eddy current problems using the magnetic vector potential can be found in [13]. Electromagnetic forces acting on mechanical structure were computed by Moon [14]. Numerical analysis and design of coils was performed in work [15].

The progress in simulation of particular fields stimulated the development of numerical methods and computational technologies for multi-physical phenomena, including coupled fields and thermal effects [5]. Various coupling mechanisms in a different context, such as magnetic field with electrical circuits [16], thermo-electro-magnetic field coupling [17], thermo-electro-structural analysis [18], electromagneto-thermoelasticity [19] and multiphase flows

[20] are meant by the term "coupled analysis". The full simulation of electro-magnetic devices [10] involves the solution of linear or non-linear partial differential equations (PDE). There is a well-known interaction among the electromagnetic field distribution, heating and the mechanics of the device. The induced Joule heating and generated thermal fields have been the subject of investigation for a long time [6]. Experimental measurements showed that the variation of temperature can reach several hundreds of degrees in pulsed solenoids [21]. High temperature fields influence material properties of the solenoid [22]. The investigation of thermal fields is successively performed by the FEM [8]. Temperature-dependent material properties couple several physical fields and present a challenge to non-linear FEM analysis.

The available numerical analyses are strongly dependent on the application. Paretti et. al. [23] numerically investigated the induction heating problem. Thermal processes in superconducting coils were explored by employing 3D computations [15]. Coupled thermo-electromagnetic analysis was applied to other superconductors [17]. Carbon to cast iron electrical contact resistance was investigated using the coupled thermo-electro-structural FEM model [18]. Numerical analysis based on the analytical simplifications was extensively applied in electromagneto-thermoelasticity [23]. The newest achievements have made a strong impact on the development of finite element codes [24] containing multi-physical utilities for magneto-thermal analysis. The major investigations have been, and continue to be, focused on performing coupled non-linear analysis including several physical fields and temperature-dependent material properties.

In this paper, the numerical thermal analysis of pulsed power magnetic field generators is presented. The coupled magneto-thermal model is employed for prediction of temperature-dependent material properties and investigation of non-linear thermal effects. An outline of the paper is as follows. Section 2 describes the mathematical model of the problem under consideration. Section 3 presents a coupled FEM formulation. Numerical behaviour of magnetic fields is validated by comparison with experimental measurements, and the results of thermal analysis are discussed in Section 4. The investigated generator is described in Section 5. Conclusions are drawn in Section 6.

2. THE MATHEMATICAL MODEL

The first law of thermodynamics and Fourier's law of heat conduction describe thermal fields. Neglecting the velocity for the mass transport of heat the parabolic equation of temperature conduction is considered [6]:

$$\rho c(T)\frac{\partial T}{\partial t} - \nabla \cdot [K(T)]\nabla T = \hat{q}, \qquad (1)$$

here T is the temperature, r is the density, $c(T)$ is specific heat which might depend on the temperature, $[K(T)]$ is the conductivity matrix which might be orthotropic or temperature-dependent, $\hat{q}$ is the heat generation rate per unit volume. It is assumed that all effects are in the Cartesian reference frame, where ∇ represents the gradient and $\nabla\cdot$ represents the divergence operator. The equation (1) is non-linear and requires an iterative solution procedure. In some cases specific heat and conductivity are assumed to be constant and the results of linear thermal analysis can be sufficiently accurate. Non-linear effects caused by the temperature-dependent material properties $c(T)$ and $[K(T)]$ can be very significant when a large variation of temperature occurs [25].

The standard Newman's boundary conditions are prescribed in the considered analysis. The heat flow acting over surface S is specified:

$$n \cdot [K(T)] = q, \qquad (2)$$

here n is the normal vector, q is specified heat flow, which vanishes in the case of thermally isolated surfaces. The initial conditions should be prescribed on whole solution domain:

$$T = T_{ini}, \qquad (3)$$

here T_{ini} is the initial temperature of the continuum.

In the performed analysis, the heat source $\hat{q}$ is computed from the induced Joule heat:

$$Q^J = RJ \cdot J, \qquad (4)$$

here R is electric resistivity and J is the total current density. The Joule heat is obtained performing coupled magneto-thermal analysis [24]. It serves as the coupling term as well as the main thermal load.

In the following transient magnetic analysis, for the given current density the temporal and spatial evolution of magnetic flux density B is described by the Maxwell equations [10]:

$$\nabla \times H = J, \qquad (5)$$

$$\nabla \cdot B = 0, \qquad (6)$$

$$\nabla \times E = -\frac{\partial B}{\partial t}, \qquad (7)$$

where H is magnetic field intensity vector, E is electric field intensity vector. Neglecting permanent magnets, the constitutive relation is

$$H = [\nu]B, \qquad (8)$$

where $[\nu]$ is the reluctivity matrix, which is the inverse of magnetic permeability $[\mu]$. In ferromagnetic regions the constitutive relation (8) is represented by a non-linear curve. Reflecting the magnetic properties of the media, the Maxwell equations (5–7) can be governed by introducing a potential field approach [13], which allows the investigated field to be expressed as

$$B = \nabla \times A, \qquad (9)$$

$$E = -\frac{\partial A}{\partial t}, \qquad (10)$$

where A is the magnetic vector potential. Equations (1, 5–7) form the basis for coupled magneto-thermal analysis.

2. COUPLED FEM FORMULATION

The numerical model of the performed magneto-thermal analysis is based on the finite element method [8]. The application of the Galerkin weighted residual method to governing equations results in a system of algebraic finite element equations that can be expressed in the matrix form [24]:

$$\begin{bmatrix} [C^{M}] & [0] \\ [0] & [C^{t}(T)] \end{bmatrix} \begin{Bmatrix} \dot{A} \\ \dot{T} \end{Bmatrix} + \begin{bmatrix} [K^{M}(A)] & [0] \\ [0] & [D^{t}(T)] \end{bmatrix} \begin{Bmatrix} A \\ T \end{Bmatrix} = \begin{Bmatrix} J \\ Q^{J}(A) \end{Bmatrix}, \quad (11)$$

where $\boldsymbol{A}$ and $\boldsymbol{T}$ are unknown nodal values of the magnetic vector potential and temperature; $\dot{A}$ and $\dot{T}$ are their first derivatives. $[C^M]$ and $[K^M(A)]$ are magnetic matrices, while J_s is the given source current density. The finite element coefficient matrix $[K^M_{(A)}]$ for magnetic analysis consists of several parts. One of them evaluates the magnetic non-linearity occurring in ferromagnetic regions. The matrix $[C^M]$ describes eddy currents that might be induced in parts of the construction fabricated from steel. The temperature-dependent matrices $[C^t(T)]$ and $[D^t(T)]$ are a specific heat (thermal damping) matrix and the diffusion conductivity matrix, respectively. $Q^J(A)$ is the thermal source vector computed from the Joule heat (4). The magnetic problem is coupled with thermal analysis by the induced Joule heat vector $Q^J(A)$. The detailed expressions of the outlined matrices can be found in reference [27]. In the current work, non-linear magneto-thermal analysis is performed in the coupled fashion considering all advantages of multi-physical approach.

4. DESCRIPTION OF PULSED GENERATOR

The pulsed laboratory device [4] generating half-period sinus-shaped magnetic field pulses of 0.15–2 ms duration and with the amplitudes up to 50 T in a 12 mm diameter bore was investigated numerically. The solenoid was fabricated using multi-layer technology and included 6 layers of copper wire wound in 18 turns in each layer. During the rolling, each layer was insulated with the epoxy-glass fibre composite. The inside diameter of the coil was d = 12 mm and the outside diameter was D = 32 mm, while the length l = 30 mm. The coil was placed into an external hollow steel cylinder reinforcement. The inside diameter of the cylinder was 40 mm and the outside diameter 50 mm, the length being 40 mm. The region of coil windings was separated from the steel cylinder by a 4 mm thick glass fibre composite layer. The fabricated coil was mounted inside an 11 mm thick steel security container to avoid any damage of the laboratory system.

The axisymmetric formulation of the coupled problem (11) is investigated in coil analysis. Due to the axial symmetry only a quarter of the coil section with 2D solution domain defined in OXY plane is considered. The geometry of the quarter section of the device

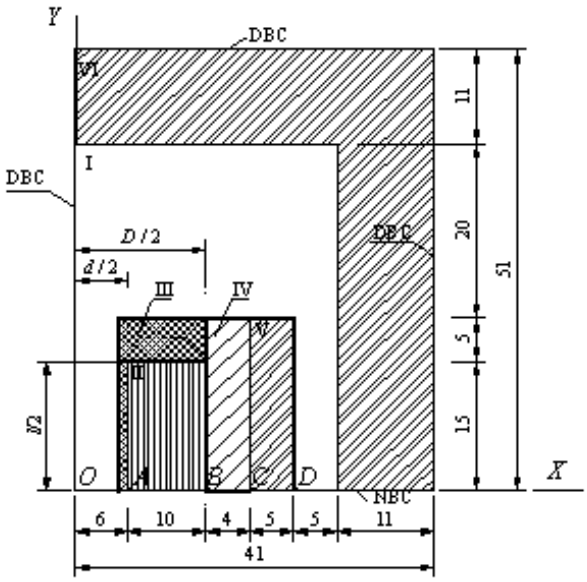

Fig. 1. The geometry of the solution domain and boundary conditions

is depicted in Fig. 1. In this axisymmetric case, only the component A_z of the potential vector $\boldsymbol{A}$ is not equal to zero. The standard boundary conditions are prescribed on the boundaries of the solution domain. The natural Newman's boundary conditions (NBC) for the magnetic potential are prescribed on OX axis. The Dirichlet boundary conditions (DBC) are specified on the rotating symmetry axis OY and on the external part of the solution domain. The zero heat flow (2) is specified on all boundaries, because the steel security container is isolated. The initial temperature (3) is 20 °C.

The magnetic load is created by the source current density:

$$J_s(t) = \frac{N \cdot I(t)}{A}, \quad (12)$$

here N is the number of half turns, A is a half of the cross-section area, while I is the prescribed source current.

Finally, the solution domain is replaced by a rectangular box with the dimensions of 41 ´ 51 mm. It consists of six different regions: air (region I), windings of the coil (region II), epoxy-textolite (region III), epoxy-glass separation layer (region IV), steel hollow cylinder reinforcement (region V) and steel security container (region VI). Magnetic properties of the regions are predefined by the relative magnetic permeability $\mu = 1$ for all materials except steel, where non-linear magnetic properties are defined by the material property curve [25]. The non-linear behaviour of the magnetic field in the investigated steel could be observed when the magnetic flux density B_y reaches the value equal to 1.5 T. The electric resistivity is defined in the steel cylinder $R = 69 \cdot 10^{-8}$ Ωm and in the copper windings area $R = 1.67 \cdot 10^{-8}$ Ωm.

The thermal material properties are defined as follows. The specific heat and conductivity of air, glass-fibre and textolite weekly depends on the temperature, therefore, they are defined as constants. The density of the air ρ = 1.29 kg/m^3, the specific heat c = 1008 J/kgK, the conductivity k = 0.025 W/mK. The density of the epoxy-glass-fibre ρ = 2600 kg/m^3, the specific heat c = 737 J/kgK, the conductivity k = 0.045 W/mK. The density of the textolite ρ = 1400 kg/m^3, the specific heat c=707 J/kgK, the conductivity k = 0.043 W/mK. The properties of the steel applied to the cylinder reinforcement are assumed to be constant, because in the cylinder the temperature changes do not exceed 5 °C. The density of the steel ρ = 7850 kg/m^3, the specific heat c = 1270 J/kgK, the conductivity k = 45 W/mK. The coil windings area presenting a layered copper-epoxy-glass composite is modelled assuming that it is a homogeneous material. The material properties of the homogeneous region are computed considering assumptions of the composite theory [26]. The averaged density of a layered composite ρ = 6695 kg/m^3. The averaged specific heat curve is plotted in Fig. 2. The copper occupies 60% of the area, therefore, the averaged curve is closer to the specific heat of copper. The thermal conductivity curve is also averaged, but the influence of its variation on the thermal process and numerical results are negligible. The mechanical material properties can be found in paper [27].

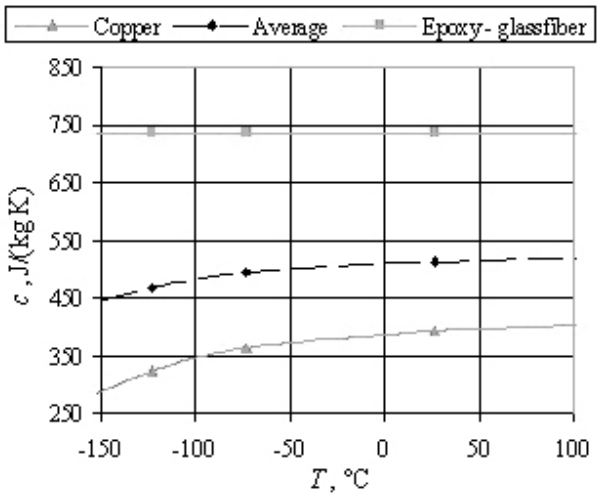

Fig. 2. The averaged specific heat in the coil winding area

5. NUMERICAL RESULTS AND DISCUSSION

The designed laboratory system generates pulsed magnetic fields, therefore, it is very important to perform transient magnetic analysis (5–7) accurately and to capture essential transient effects. The results of the numerical analysis are verified by experimental measurements. The short magnetic field pulses are generated and accurately measured with available experimental equipment in [4]. The variation of the experimentally measured current in time is plotted in Fig. 3a. Three

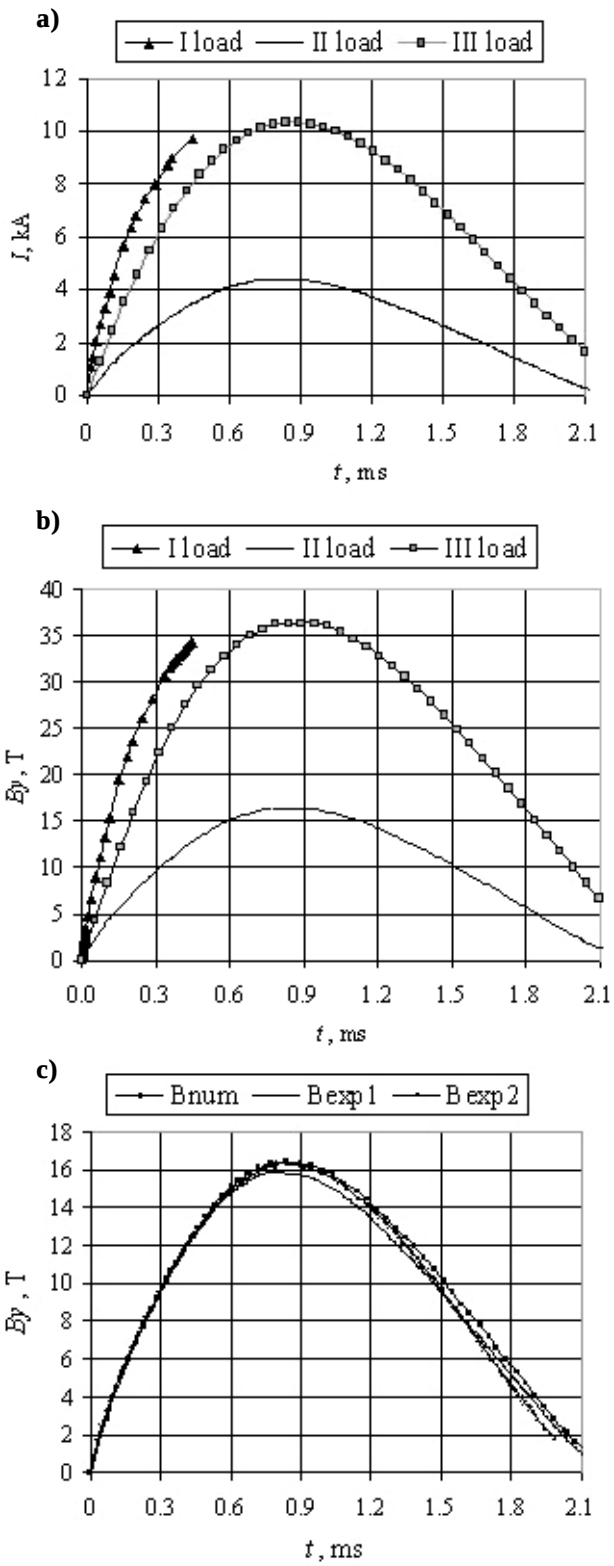

Fig. 3. Results of magnetic analysis: (*a*) three current loads, (*b*) the time evolution of magnetic flux density in the central point of the coil, (*c*) magnetic flux density generated by the second load: numerical results (Bnum) and experimental measurements (Bexp1, Bexp2)

different current loads are investigated. The first load simulates the destructive coil producing short-circuiting of windings and a very fast discharge of electric

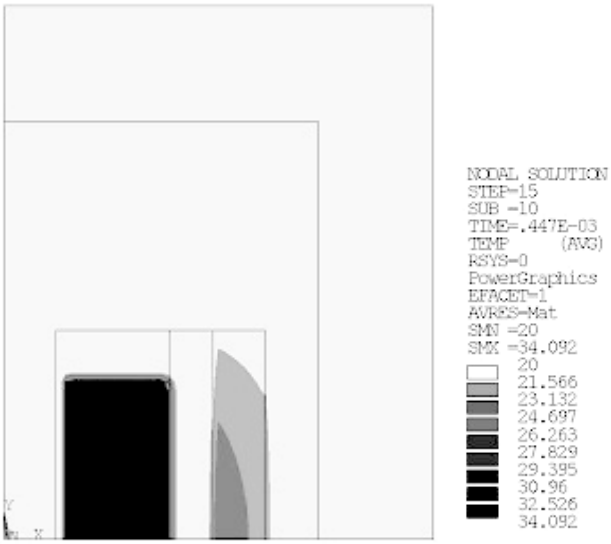

Fig. 4. Distribution of temperature at the end of the first load t = 0.447 ms

energy. The second load represents the current pulse with a low amplitude of 4.1 kA resulting in a magnetic field of 16 T. The third load simulates the high magnetic field of 36 T in the multishoot coil. The experimental data were preceded and incorporated in the numerical magnetic analysis as the source current density $\boldsymbol{J}_s$. The results of magnetic analysis are plotted in Fig. 3b. The time evolution of magnetic flux density in the central point of the coil is presented. A quantitative comparison of numerical results (Bnum) and experimental measurements (Bexp1, Bexp2) is shown in Fig. 3c. In the central point of the coil, the numerical analysis accurately predicts the pulse of magnetic field. The error is less than 4%. The experimental measurements obtained by using different magnetic field sensors [4] are of similar accuracy.

The temperature fields are computed by using FEM analysis. The temperature distribution at the end of the first current load is shown in Fig. 4. The small increase of temperature can be explained by the short time of the first load (0.447 ms). The highest values of the temperature are concentrated in the area of coil windings. The temperature rises by 14 °C in this region, while in the steel cylinder its variation is only 4.6 °C. The pulse time is very short and the influence of conduction processes to final results is quite small. The small conductivity values of epoxy-glass fibre and textolite also play an important role in the final distribution of the temperature. The magnitude of the prescribed source current density is significantly larger than that of the induced eddy current density. Thus, in the area of coil windings a bigger quantity of the Joule heat is induced and the resulting temperature is higher.

The time evolution of the temperature is shown in Fig. 5. The values of the temperature are examined in one point of coil windings area, because the temperature is constant in the whole region. In the steel cylinder the point with the maximal temperature is cho-

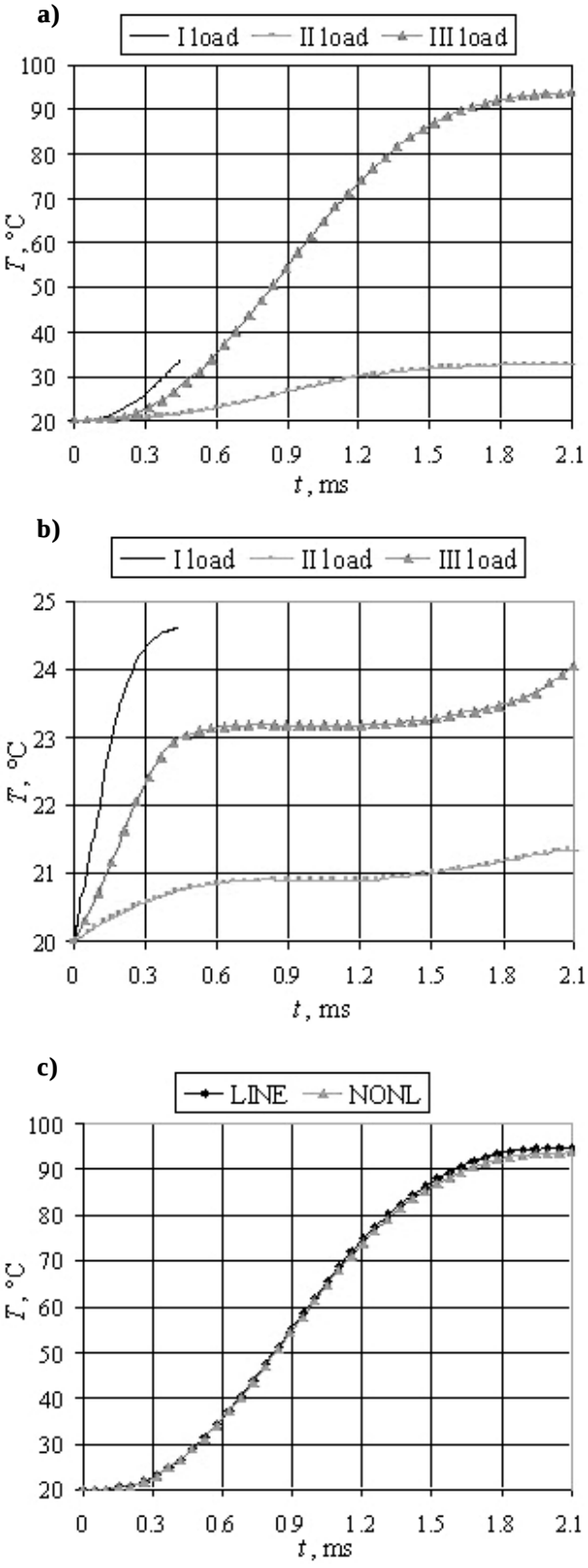

Fig. 5. Results of thermal analysis obtained by using three current loads: (*a*) time evolution of temperature in the area of coil windings, (*b*) time evolution of temperature in the point of the steel cylinder, (*c*) quantitative comparison of results obtained by linear (LINE) and non-linear (NONL) thermal analyses in the coil windings area

sen. The numerical results obtained by using three loads are investigated. The highest values of the temperature were observed in the case of the third load. The amplitude of the current pulse is similar to that of the first load, but the duration of the pulse of the third load is longer. In the area of coil windings, the fastest rise of temperature is observed in the middle of the pulse (about 0.8 ms) when the values of the source current are the highest. In the steel cylinder the temperature evolution character is totally different. This is due to a different nature of the induced eddy currents. The large eddy currents are measured when the derivative of the magnetic field potential in time is large. It is observed at the beginning and at the end of the pulse. Thus, the first load produces the largest variations of temperature in the steel cylinder because of the shortest rise time of the current pulse.

Figure 5c shows a quantitative comparison of the results obtained by different thermal analyses. The first curve illustrates the linear thermal analysis. The conductivity and specific heat are treated as averaged constants that do not depend on the temperature. At the end of the third load the temperature raised up to 94 °C. The values of thermal properties at 94 °C are different than that at 20 °C. In order to evaluate the error of the linear thermal analysis and the influence of temperature-dependent conductivity and specific heat, the non-linear thermal analysis was performed. The second curve shows that the values of temperature obtained by non-linear computations are lower. This is due to a small increase of specific heat at the study temperatures (Fig. 2). The induced Joule heat does not depend on the type of analysis. Thus, larger values of specific heat at the end of the load cause lower values of the temperature in the area of coil windings. In the current investigations the error of linear analysis does not exceed 1.5%.

3. CONCLUSIONS

In the frame of the current research, coupled FEM analysis has been applied for investigating thermal fields induced in a pulsed power magnetic field generator. The analysis was based on the coupled magneto-thermal model available in ANSYS software. The accuracy of magnetic analysis has been verified by a comparison with the experimental measurements. The non-linear thermal analysis considered the variation of temperature-dependent material properties. In the destructive coils generating magnetic fields up to 36 T, the variation of temperature is small and has no influence on temperature-dependent material properties. In the multishoot coils the complete magnetic field pulse of 2.1 ms duration with amplitudes up to 36 T raises the temperature of the coil windings area by 74 °C. Mechanical analysis of the device thermal loads should be considered, but the variation of mechanical material properties in temperature can be neglected. A quantitative comparison of the results obtained by the linear and non-linear analyses has been performed. Numerical experiments have shown that the temperature values of the non-linear thermal analysis are by 1.5% lower than those of the linear solution. In the temperature interval studied, the results of linear thermal analysis were sufficiently accurate and non-linear thermal effects could be neglected.

ACKNOWLEDGEMENTS

The work was supported by the Lithuanian Science and Studies Foundation under the contract No. K-058.

Received 1 September 2004

References

1. Knoepfel H. Pulsed Magnetic Fields. North-Holland Publishing Company. Amsterdam, 1970.
2. Miya K., Uesaka M., Yoshida Y. Applied electromagnetics research and application // Progress in Nuclear Energy. 1998. Vol. 32. No. 1–2. P. 179–194.
3. Herlach F. Laboratory electromagnets – from Oersted to megagauss // Physica B. 2002. Vol. 319. P. 321–329.
4. Balevièius S., Novickij J., Abrutis A., Kiprijanoviè O., Anisimovas F., Ðimkevièius È., Stankeviè V., Vengalis B., Þurauskienë N., Altgilbers L.L. Manganite based strong magnetic field sensors used for magnetocumulative generators // Materials Science Forum. Trans Tech Publications Ltd., Switzerland. 2002. Vol. 384–385. P. 297–300.
5. Gupta K.K., Meek J. L. Finite Element Multidisciplinary Analysis. AIAA, New York, 2000.
6. Schneider P. J. Conduction Heat Transfer. 2nd ed. Addison-Wesley Publishing Co., Reading, MA, 1957.
7. Nicholson D.W., Finite Element Analysis: Thermomechanics of Solids. CRC Press, Boca Raton, 2003.
8. Zienkiewicz O. C., Taylor R. L. The Finite Element Method. Vol. 1–3. 5th ed. Butterworth Heinemann, London, 2000.
9. Lewis R. W., Morgan K., Thomas H. R., Seetharamu K. N. The Finite Element Method in Heat Transfer Analysis. J. Wiley & Sons, New York, 1996.
10. Silvester P., Ferrari R. L. Finite Elements for Electrical Engineers. 3rd ed. Cambridge University Press, Cambridge, 1996.
11. Demerdash N. A., Nehl T. W., Fouad F. A., Mohammed O. A. Three-dimensional finite element vector potential formulation of magnetic fields in electrical apparatus // IEEE Transactions on Power Apparatus and Systems. 1981. Vol. PAS-100. No. 8. P. 4104–4111.
12. Gyimesi M., Lavers D., Pawlak T., Ostergaard D. Application of the general potential formulation in the ANSYS program // IEEE Transactions on Magnetics. 1993. Vol. 29. P. 1345–1347.
13. Bíró O., Preis K. On the use of the magnetic vector potential in the finite element analysis of three-dimensional eddy currents // IEEE Transactions on Magnetics. 1989. Vol. 25. No. 4. P. 3145–3159.

14. Moon F. C. Magneto-Solid Mechanics. New York, John Wiley and Sons Inc., 1984.
15. Netter D., Leveque J., Rezzoug A., Caron J. P., Sargos F. M. 3D-computation of a thermal process in a superconducting coil // IEEE Transactions on Magnetics. 1995. Vol. 31. No. 6. P. 4127–4129.
16. De Gersem H., Mertens R., Lahaye D., Vandewalle S., Hameyer K. Solution strategies for transient, field-circuit coupled systems // IEEE Transactions on Magnetics. 2000. Vol. 36. No. 4. P. 1531–1534.
17. Shiraishi R., Demachi K., Uesaka M. Numerical simulation of coupled problem of electromagnetic field and heat conduction in superconducting magnetic bearing // Physica C: Superconductivity. 2003. Vol. 392–396. Part 1. P. 734–738.
18. Richard D., Fafard M., Lacroix R., Cléry P., Maltais Y. Carbon to cast iron electrical contact resistance constitutive model for finite element analysis // Journal of Materials Processing Technology. 2003. Vol. 132. No. 1–3. P. 119–131.
19. Tianhu H., Yapeng S., Xiaogeng T. A two-dimensional generalized thermal shock problem for a half-space in electromagneto-thermoelasticity // Int. J. Engineering Science. 2004. Vol. 42. No. 8–9. P. 809–823.
20. Kaèeniauskas A. Two-phase flow modelling by the level set method and finite elements // Energetika. 2000. Vol. 4. No. 1. P. 22–31.
21. Montgomery D. Solenoid Magnet Design. J. Wiley & Sons, New York, 1969.
22. Noto K., Oka T., Yokoyama K., Katagiri K., Fujishiro H., Okada H., Nakazawa H., Muralidhar M., Murakami M. Thermal and mechanical properties of high T_c bulk superconductors and their applications // Physica C. 2003. Vol. 392–396. P. 677–683.
23. Parietti C., Rappaz J. A quasi-statis two-dimensiomal induction heating: II. Numerical analysis // Mathematical Methods and Models in Applied Sciences. 1999. Vol. 9. P. 1333–1350.
24. ANSYS Theory Reference. 8th ed. SAS IP INC., 1997.
25. Washburn E. W. (ed.). International Critical Tables of Numerical Data, Physics, Chemistry and Technology. Knowel, New York, 2003.
26. Berthelot J. M. Composite Materials. Mechanical Behavior and Structural Analysis. Springer-Verlag, New York, 1999.
27. Balevièius S., Þurauskienë N., Novickij J., Kaèeniauskas A., Kaèianauskas R., Stupak E. Decoupled algorithm for coupled magneto-mechanical analysis of coils by the FEM software // J. Information technology and Control. 2003. Vol. 3. No. 28. P. 54–61.

Vincas Ðnirpûnas, Eugeniuð Stupak, Rimantas Kaèianauskas, Arnas Kaèeniauskas, Jurij Novickij

ÐILUMINË IMPULSINIØ MAGNETINIØ LAUKØ GENERATORIAUS ANALIZË BAIGTINIØ ELEMENTØ METODU

Santrauka

Pateikiama impulsiniø magnetiniø laukø generatoriuje susidaranèiø temperatûros laukø skaitinë analizë. Vilniaus stipriøjø magnetiniø laukø centre sukurta laboratorinë áranga generuoja sinusoidinius 2 ms trukmës magnetinio lauko impulsus, kuriø amplitudë siekia 50 T. Didþiausia impulsinio generatoriaus galia lygi 15 MW. Skaitinë analizë, pagrásta baigtiniø elementø metodu, modeliuoja nestacionarius magnetinius procesus, indukuotà ðilumos kieká ir temperatûros laukus impulsiniame generatoriuje. Netiesinë ðiluminë analizë atliekama ávertinant savitosios ðilumos ir ðilumos laidumo koeficientø priklausomybæ nuo temperatûros. Skaitiniai magnetiniø laukø rezultatai palyginti su eksperimentiniais duomenimis. Temperatûros laukø analizë skirta ávertinti medþiagø savybiø, priklausanèiø nuo temperatûros, koeficientø pokyèiams.

Raktaþodþiai: ðiluminë analizë, susieta magnetoterminë analizë, impulsiniai magnetiniø laukø generatoriai, baigtiniø elementø metodas

Винцас Шнирпунас, Евгений Ступак, Римантас Качянаускас, Арнас Каченяускас, Юрий Новицкий

ТЕПЛОВОЙ АНАЛИЗ ИМПУЛЬСНОГО ГЕНЕРАТОРА МАГНИТНЫХ ПОЛЕЙ МЕТОДОМ КОНЕЧНЫХ ЭЛЕМЕНТОВ

Резюме

Приводится тепловой анализ импульсного генератора магнитных полей методом конечных элементов. В Вильнюсском центре сильных магнитных полей создана лабораторная система, генерирующая синусоидные магнитные импульсы длиной 2 мс, амплитуда которых достигает 50 Т. Пиковая мощность импульсного генератора составляет 15 MW. Численный анализ, обоснованный методом конечных элементов, моделирует нестационарные магнитные поля, выделяющие тепло в импульсном генераторе. Нелинейный тепловой анализ учитывает зависимость коэффициентов удельной теплоемкости и теплопроводности от температуры. Результаты численного магнитного анализа сравнены с экспериментальными величинами. Тепловой анализ помог определить значения коэффициентов от температуры зависящих свойств материалов.

Êëþ÷åâûå ñëîâà: òåïëîâîé àíàëèç, ñâÿçàííûé ìàãíèòîóïðîâîé àíàëèç, èìïóëüñíûé ãåíåðàòîð ìàãíèòíûõ ïîëåé, ìåòîä êîíå÷íûõ ýëåìåíòîâ